JOURNAL OF MATERIALS SCIENCE 20 (1985) 1471–1479

Metastable phases in amorphous metals with emphasis on Fe_3B

JOHN L. WALTER, AMI E. BERKOWITZ
Metallurgy Laboratory, GE Research and Development Centre, PO Box 8, Schnectady, New York 12301, USA

The amorphous metallic state may be obtained by a number of methods such as vapour deposition, ion-beam implantation and mixing, and by rapid solidification of liquid metals. New metastable phases may be derived from the amorphous state. This paper reviews the type and nature of some of these metastable phases. In particular, it will be shown that the metastable bc tetragonal Fe_3B phase may be related to the presence of simple unit cells in the amorphous phase. Fe_3B may also be found in a conventionally cast material.

1. Introduction

Metastable phases may occur only when a metal is cooled too rapidly for the equilibrium phases to nucleate and grow upon solidification. These phases may take the form of extended solid solutions or "new phases". An example of the former case in the Cd–In system is the intermediate fcc α-phase, stable between 5 and 20 at % In and above 290 K which was extended to 89 at % by splat cooling [1]. The "new" phase also may be defined as a phase which is not known to exist in stable form by any combination of alloy concentration, pressure, or temperature. Thus, as more experimentation is carried out, the number of phases now known as metastable must inevitably decrease as knowledge of stable phase fields increases. A case in point may be the metastable bc tetragonal Fe_3B phase which will be discussed later. Perhaps the ultimate in metastable phases is the amorphous state achieved at such high cooling rates from the liquid that crystallization does not have time to occur before the melt becomes solid.

Alloy systems with restricted terminal solid solubility, with atom size differences greater than about 10% and with limited tendency to form intermediate phases at equilibrium are most likely to form metastable phases [2].

This paper will consider only metastable phases arising from the decomposition of the amorphous phase.

2. The amorphous phase

Amorphous metallic alloys have been prepared by processes such as liquid quenching [3], vapour deposition, "laser glazing [4–8]," and ion-beam implantation and mixing [9, 10]. These methods of preparation have in common the fact that the atoms, once delivered to a substrate, cannot rearrange themselves over long distances and must remain more-or-less randomly distributed, that is, are in the glassy or amorphous state. In forming a material from the melt as in splat cooling, ribbon casting, spark erosion, or by laser glazing, the cooling rate is so rapid that the atoms do not have time to diffuse before the viscosity of the solid becomes too high for diffusion to occur in reasonable time [3, 10]. Thus, crystallization is avoided since the atoms cannot form nuclei or the growth rate of any cast-in nuclei is too low to permit growth to the point where crystals are observable.

Vapour deposition or vapour quenching is the condensation of vapour on a substrate which is at a temperature low enough that the attached atoms are not mobile and the heat of condensation is absorbed by the substrate so that there is no appreciable rise in temperature [11].

Ion bombardment destroys the crystallinity of the target material by causing displacement of the atoms. Because of the very rapid effective quenching rate achieved in a thermal spike during particle

0022–2461/85 $03.00 + .12

bombardment, the matrix may be thoroughly randomized. Similarly, amorphous alloys may be obtained by ion bombardment of multilayered samples to produce the desired composition in the amorphous condition [12].

The very randomness of the amorphous matrix may then set the stage for crystallization of metastable phases because the state of chemical short range order would provide the combination of atoms to nucleate the nonequilibrium phase. That is, the metastable phase will generally have a composition close to that of the amorphous matrix. The metastable phase is known as such because it will decompose to a stable phase or phases with time or with increased temperature. The metastable phase may be relatively stable once nucleated in the amorphous matrix or it may transform to another phase that would not have been expected as in the case of the binary alloy Fe–P which will be discussed later.

3. Vapour deposited alloys

Perhaps the most effective process for preparing alloy systems with metastable phases is that of vapour deposition or sputtering wherein thin layers of different metals are evaporated or coevaporated upon a substrate. These methods can produce compositions far from equilibrium or which could not be made by melting without separation of the elements. An interesting alloy system is Au–Si which may be made as amorphous thin films [13]. This alloy crystallizes at room temperature. The decomposition reaction begins with the dissociation of the amorphous alloy into an amorphous μ-phase and an amorphous silicon phase via the fast diffusion of gold. The two amorphous phases may consist of a silicon rich area with interstitial gold atoms and gold-rich areas (amorphous μ) having a structure similar to that of the crystalline μ-phase [13]. A schematic free energy diagram [13] is shown in Fig. 1. In this case the free energy in the amorphous state is taken as that of a virtual liquid with two minima corresponding to the amorphous silicon and amorphous μ. This diagram is supported by analysis of the diffraction patterns of the film. That is, near $AuSi_3$, the TE diffraction pattern might be generated by superposing those obtained with gold-rich and silicon-rich amorphous alloys. Crystallization into the metastable phase would be by diffusionless transformation of silicon-rich areas into silicon and μ without changes in the

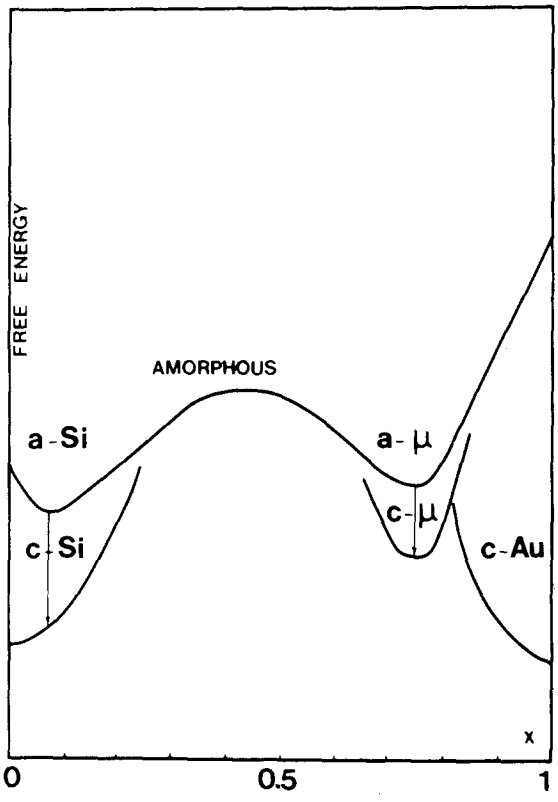

Figure 1 Schematic free energy diagram of the amorphous state of Au–Si. From [13].

compositional variations. The alloy crystallizes at room temperature, first to the metastable μ-phase and, with time at RT, the μ-phase decomposes to gold and silicon. The process may be followed by observing the colour change from silver to gold within hours.

The μ-phase grows as fairly large striated crystals into the amorphous matrix. Transmission electron diffraction patterns show the μ-phase to be orthorhomic with parameters $a = 1.29$, $b = 0.745$, and $c = 1.16$ nm [13]. The μ-phase appears alone only when the composition $Au_{75}Si_{25}$ crystallizes. At $Au_{27}Si_{73}$, both crystalline μ and crystalline silicon are present on crystallization.

Another alloy system without intermetallic compounds is Cu–Ag [11]. For instance, the $Cu_{46}Ag_{54}$ film is amorphous on vapour deposition at 80 K. Upon annealing for 1.5 h at 380 K, a single metastable f c c phase with the lattice constant of 0.398 nm occurs. The microstructure consists of 5.0 nm particles. Annealing at 600 K causes the metastable phase to decompose to the two equilibrium phases silver and copper. The formation of the metastable phase is preferred

over that of the two phases because diffusion over relatively long distances would have to take place to form the silver and gold phases. On the other hand, formation of the ordered compound structure requires diffusion only over a few atom distances. Thus, under conditions of rapid cooling, it is easier to form a metastable phase which has the composition of the amorphous matrix than it is to form two phases quite different in composition. Vapour deposited $Co_{70}Au_{30}$ also formed the f c c metastable phase which decomposed into the two elements on further heating [11].

The metastable f c c phase may also be obtained in $Co_{83}Au_{17}$ alloys formed by vapour deposition then bombarded with xenon ions to thoroughly mix the elements [14]. The composition of the metastable f c c supersaturated substitutional solid solution is close to that of the alloy.

4. Ion beam mixing

New alloys may also be prepared by depositing a film a few tens of nanometres thick on a matrix, then mixing the two by ion bombardment to obtain the desired composition. By depositing platinum films on silicon and bombarding with xenon ions, the platinum film is mixed with silicon atoms and a silicon-rich Pt–Si mixed layer is formed [15]. The layer can be amorphous. Annealing for 10 min at 400° C produces a uniform layer with a silicon to platinum concentration ratio close to 1.5. At the same time, the metastable phase Pt_2Si_3 begins to form. This phase is hexagonal with $a = 0.3841$ and $c = 1.1924$ nm and it decomposes to orthorhombic PtSi and Si on annealing at temperatures above 500° C. It is concluded that the amorphous state is a prerequisite for the formation of metastable Pt_2Si_3 and it is necessary to have the composition of the amorphous phase close to that of the compound.

Au–Si alloys may also be made amorphous by ion-beam mixing (as well as by quenching from the melt). The amorphous nature of the ion-beam mixed alloy is likely caused by a beam-enhanced interdiffusion mechanism. The interdiffusion occurs within the collision cascade volumes produced by the incident ions. The greater the number of cascades, the more thorough the intermixing. The metastable phase arising from the amorphous matrix is hexagonal with $a = 0.938$ and $c = 1.546$ nm [16]. This phase (Au_5Si_2) apparently differs from that obtained by quenching from the melt or by thermal treatment of thin gold films on silicon.

It may be that the degree of disorder obtainable in the amorphous state by ion bombardment is greater than that obtained by melt quenching. The compound Zr_3Al can be made amorphous by bombarding with argon ions [17] but cannot be made amorphous by melt quenching.

Ion-beam mixing may also provide a measure of stability of various phases. For example, when annealed at 500° C for 2 h, rapidly quenched amorphous ribbons of $Fe_{75}B_{25}$ produce crystals of metastable Fe_3B and crystals of the equilibrium phases Fe_2B and α-Fe. When bombarded with 4 MeV argon ions at 22° C, the metastable Fe_3B crystals were converted to the amorphous state at between 0.11 and 0.3 displacements per atom (dpa) [18]. Fig. 2 shows the transmission electron diffraction patterns. The Fe_2B phase required between 1.5 and 2.5 dpa to become amorphous. The α-Fe disappears completely between 19 and 50 dpa, probably as a result of mixing the very small iron crystals into the surrounding amorphous matrix.

5. Melt quenching

Cooling from the melt should present the best opportunity to gain understanding of the factors that give rise to metastable phases in preference to stable phases. In fact, the origin of the metastable phases formed in many amorphous metals may, in certain cases, be found in the liquid alloy. In the Au–Si system, close packing exists in the liquid at concentrations of silicon near 25%. This close packing effectively accommodates the silicon atoms in "solution" [19] in the liquid implying the existence of Au–Si bonds in the close packed liquid. The formation of the metastable orthorhomic phase from the $Au_{75}Si_{25}$ amorphous phase thus relates to the presence of such close packing in the amorphous phase which was obtained from the solidification of the liquid of this composition. The tendency for close packing would also be greater, the lower the temperature of the liquid, as would be the case for eutectic alloys. Thus, the lower the liquid temperature, the greater would be the tendency to form an ordered amorphous phase from which would nucleate a new phase. This chemical short range order (CSRO) of the melt should vary with the melt temperature leading to the formation of different metastable phases from the same composition of liquid. For instance, Au–Ge eutectic melts quenched from 480, 550 and

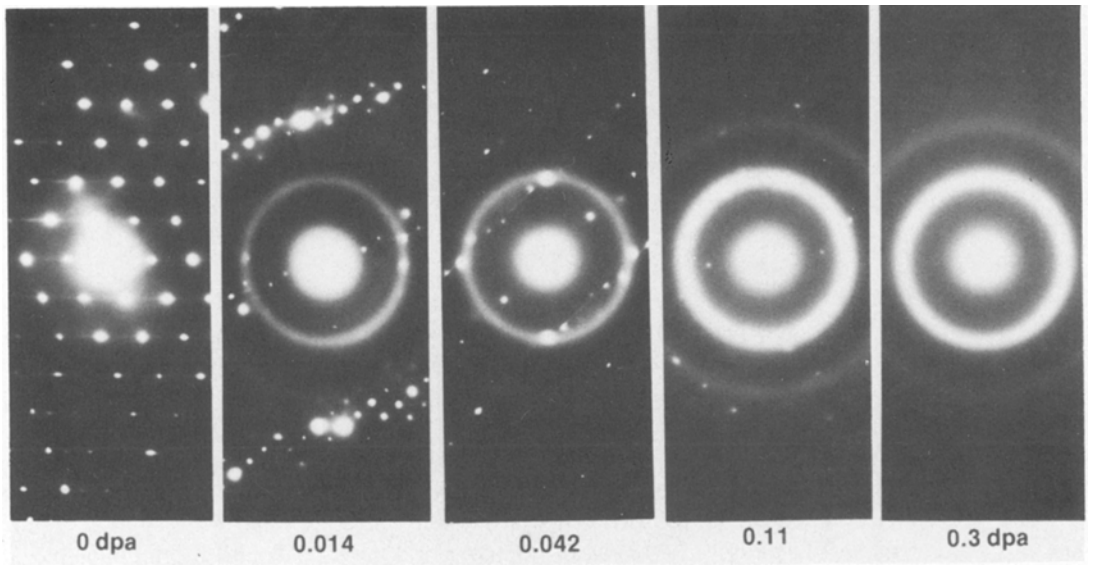

Figure 2 Crystalline to amorphous phase transformation of Fe_3B during bombardment with 4 MeV A^+ ions at 22° C. (a) 0 dpa; (b) 0.014 dpa; (c) 0.042 dpa; (d) 0.11 dpa; (e) 0.3 dpa.

800° C formed three different nonequilibrium intermediate phases [20]. The three tetragonal phases are structurally interrelated and seem to be related to differences in size of atom clusters in the liquid. It is these clusters or "domains" in the rapidly solidified amorphous $Pd_{80}Au_{20}$ that give rise to the metastable f c c crystals [21]. The amorphous structure of this alloy is closely related, in terms of palladium nearest neighbour distance, to the f c c structure of pure palladium. The domains in the amorphous matrix, by diffusion over short distances, rearrange to form the f c c structure. It is suggested that the crystals are the beginning of a metastable solid solution $Pd_{80}Au_{20}$ [21].

Most metastable phases are compounds or solid solutions. It is also possible, by rapid quenching, to produce different allotropes. For instance, near the Y–Fe eutectic composition, rapidly quenched ribbons consist of the amorphous phase with a small amount of b c c yttrium [22]. Alloys with more or less iron contained crystals of the equilibrium h c p yttrium. It is suggested that the b c c yttrium might be expected as the stable phase near the melting line [23]. If the cooling rate is sufficiently rapid to form the amorphous phase, this crystalline b c c yttria phase could not transform because of the high viscosity of the matrix. Without the amorphous phase, the metastable allotrope transforms to the stable form at high temperature and is, therefore, never observed at low temperatures.

The effect of forming a metastable phase which transforms to a stable phase under conditions which prevent it from being seen may have been encountered in the case of $Fe_{80}P_{20}$ [24]. This composition has the necessary qualifications for formation of the amorphous phase, i.e. deep eutectic with much "glass former" (phosphorus). Yet when rapidly quenched to form ribbon, it consists of nearly equiaxed crystals of Fe_3P with α-iron crystals at the grain boundaries as shown in Fig. 3. The ribbon has smooth surfaces and edges as would be expected for a good amorphous ribbon but it has a blue tint on both surfaces indicating that it was heated to at least 700° C after it left the wheel [24]. It appears that this ribbon solidified in the mostly amorphous state with a small number of crystals of the unstable eutectic α-Fe + Fe_2P included. This highly undercooled phase [25], (see phase diagram, Fig. 4) transformed to the equilibrium Fe_3P phase and the heat released caused both very rapid growth of the Fe_3P crystals and the blue tint on both surfaces of the ribbon; the ribbon transformed after leaving the wheel.

Some supposedly metastable phases may even exist under near equilibrium conditions. The b c t phase Fe_3B has been studied extensively in Fe–B amorphous alloys. It occurs in conjunction with b c c iron crystals in hypoeutectic alloys such as $Fe_{84}B_{16}$ [26] and exclusively in hypereutectic Fe–B alloys [27]. On annealing at higher temperatures,

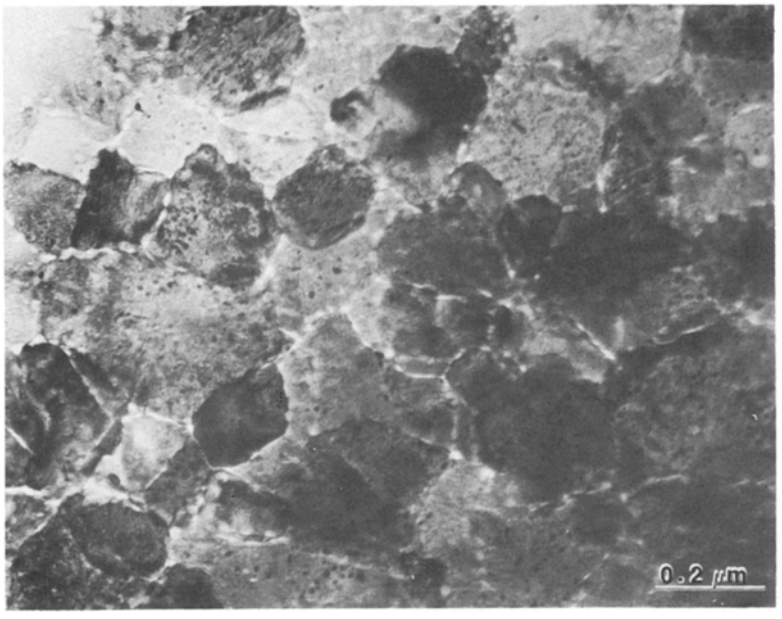

Figure 3 Transmission electron micrograph of rapidly cooled $Fe_{80}P_{20}$ ribbon.

the phase transforms to the stable phases α-Fe and Fe_2B.

The diffuse rings of transmission electron diffraction patterns of the amorphous phase $Fe_{84}B_{16}$ prepared by melt spinning were indexed; some were b c c α-iron reflections. The remainder were indexed on the basis of a simple tetragonal unit cell with $a = 0.305$ and $c = 0.262$ nm; this is the smallest unit cell which accounts for all of the reflections not identified as α-Fe [26]. The existence of such unit cells in the amorphous phase is indicated by the sharpness of the TED rings suggesting short range order involving clusters of atoms 1 to 2 nm in size. The b c t Fe_3B crystal relates to the unit cell of the amorphous phase as follows:

tetragonal amorphous phase

$a = 0.305$ nm

$c = 0.262$ nm

bc tetragonal Fe_3B crystals

$2 \times 2^{1/2}$ $\quad a = 0.863$ nm

$1\frac{2}{3}$ $\quad c = 0.437$ nm

The base of the Fe_3B crystal has an edge which is twice the face diagonal of the small tetragonal unit in the amorphous matrix and the c-axis is $1\frac{2}{3}$ the length of the amorphous cell. This relationship raises the possibility that the Fe_3B crystals were preceded by clusters of iron and boron atoms in the amorphous phase. Formation of clusters with definite ratios of iron and boron atoms results in a lowering of the free energy of the liquid because of the attractive forces of the unlike atoms [28]. Based on the atomic volume of the amorphous unit cell, there must be three boron atoms and one iron atom in the amorphous units which segregate from the Fe–B matrix to form the cluster [29]. Nucleation for crystallization then might occur as follows:

$$FeB_3 + 8Fe \rightarrow 3Fe_3B.$$

Evidence for the effect of clustering has been obtained from the alloy $Fe_{75}Si_{15}B_{10}$ [30]. Amorphous ribbons of this alloy, when heated, first form crystals of α-Fe and Fe_3Si, the latter phase being one of the equilibrium phases of this alloy. When heated at higher temperatures, the second equilibrium phase, Fe_2B appears. Particles of the same alloy were formed by spark erosion in an organic dielectric. Cooling rates for the particles were 5×10^6 K sec^{-1} for the 20 to 30 μm diameter particles and of the order of 10^9 K sec^{-1} for the smallest particles, those quenched from the vapour compared with a cooling rate of 10^6 for the 27 μm thick ribbon [30]. Crystallization characteristics [31], magnetization measurements [32] and measurements of the radial distribution function

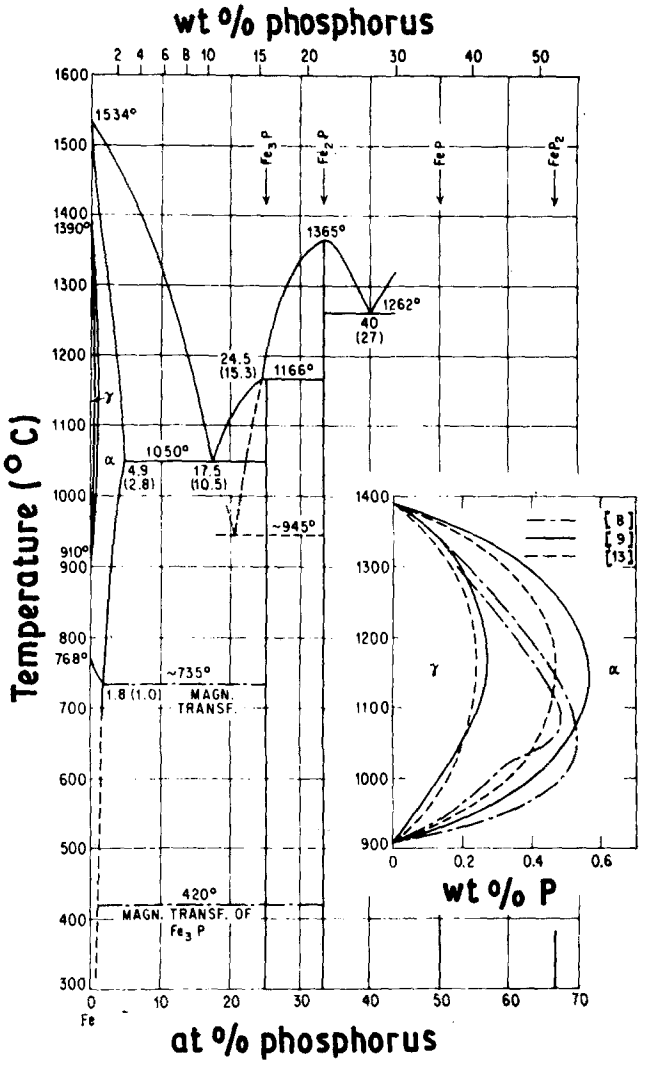

Figure 4 Fe–P phase diagram. From [25].

[33] all indicate that the chemical short range order is greater for the ribbon than for the powder particles, the difference being caused by the higher cooling rate for the particles compared with the ribbon; the reduction in CSRO also increases with decreasing particle size. Thus, there is a tendency for the iron atoms in the particles to have more boron atoms as nearest neighbours than is the case for the more chemically ordered ribbon. The clustering of boron atoms (the silicon atoms are considered to be in solid solution in the iron) could act as nuclei for growth of the b c t Fe_3B crystals which are observed to be the first crystals to form on heating the spark eroded particles of $Fe_{75}Si_{15}B_{10}$. The crystals are shown in Fig. 5, a transmission electron micrograph (TEM) of Fe_3B crystals in a 20 to 30 μm particle heated to 584° C in the differential scanning calorimeter [31]. Heating to higher temperatures causes the Fe_3B phase to be transformed to Fe_2B with Fe_3Si crystals growing simultaneously. The Fe_3B phase in this alloy is metastable. The morphology of these crystals (Fig. 5) is unlike that of b c t Fe_3B crystals in the binary Fe–B alloys.

Although the b c t Fe_3B phase is not stable at temperatures around 548° C and has been observed so far only by crystallization of amorphous alloys, it may also exist in alloys cooled at the rate of only a few hundred degrees per minute. For instance, Fig. 6 shows a TEM of a sample of $Fe_{83}B_{17}$, near the eutectic composition for this alloy. The sample was taken from a slab, 1.3 cm thick, which was cast into a copper chill mould. The eutectic consists of Fe_2B rods in a matrix of iron as one would expect and the proportions of the phases are correct. However, when the

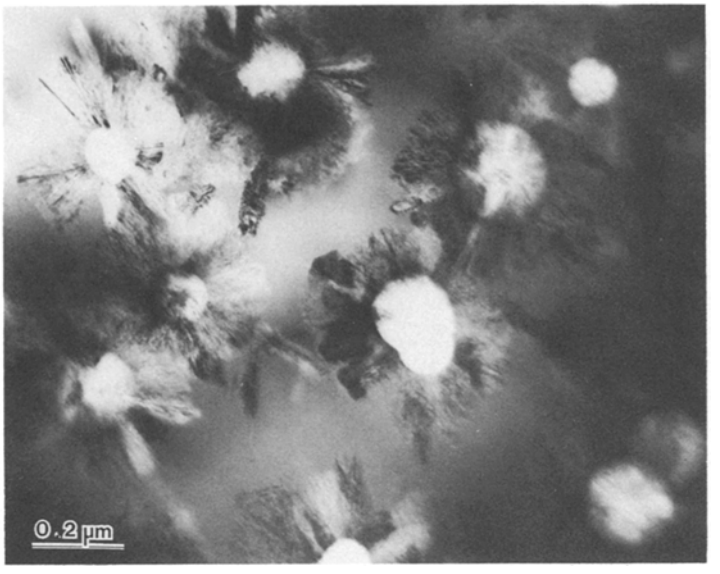

Figure 5 TEM of Fe_3B crystals in a 20 to 30 μm particle of $Fe_{75}Si_{15}B_{10}$ heated to 584° C. Diffraction pattern of crystal inset.

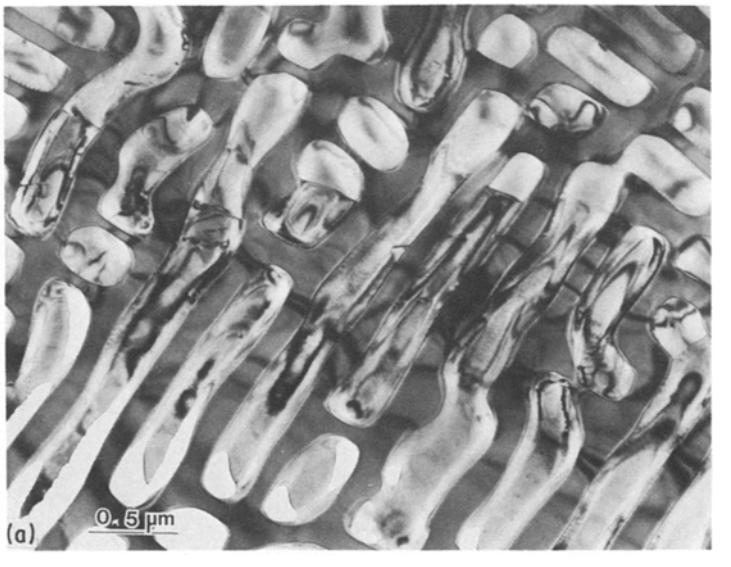

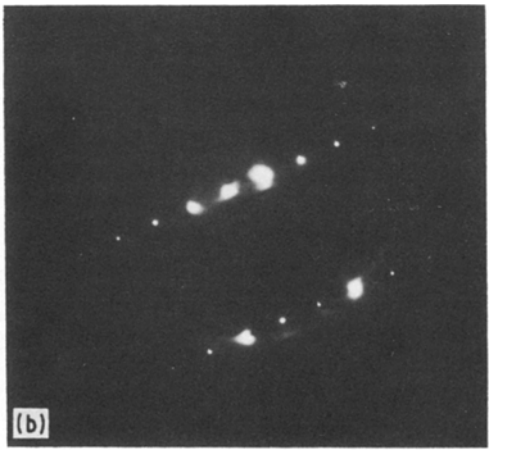

Figure 6 TEM of sample from 0.5 in thick casting of the eutectic $Fe_{83}B_{17}$ showing Fe_2B rods in the α-Fe matrix.

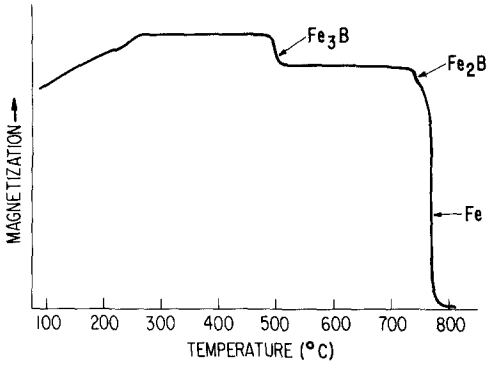

Figure 7 Magnetization of eutectic $Fe_{83}B_{17}$ casting during cooling in field of 46 Oe. Arrows indicate the Curie temperatures.

magnetization of samples of the cast ingot was measured as a function of temperature in a field of 46 Oe, there was evidence for a third phase. Fig. 7 shows the low-field cooling curve for the $Fe_{83}B_{17}$ cast alloy with the Curie temperatures for Fe, Fe_2B and b c t Fe_3B indicated thereon. Amorphous ribbons of this alloy were prepared by melt spinning and the magnetization of samples of ribbon was measured as a function of temperature. Fig. 8 shows the cooling curve for the ribbon sample in a field of 51 Oe. The Curie temperature for the Fe_3B phase is indicated by the arrow. Although the T_c of the Fe_3B phase in the ribbon differs by a few degrees from that in the casting (Fig. 7) there is no doubt that the measurement of magnetization as a function of temperature has revealed the presence of Fe_3B in the relatively slowly cooled casting of $Fe_{83}B_{17}$. It may be that the b c t Fe_3B phase will be observed only in relatively slowly cooled alloys of the eutectic composition because of the clustering of the iron and boron atoms in the liquid at the lower melt temperatures.

Other studies of the Fe–B system suggest that the metastable supersaturated solid solution of boron in α–Fe (Fe_4B) occurs along with the b c t Fe_3B crystallization [34]. The arrangements of the iron atoms around the boron atoms in the two structures are stable and resemble each other. This arrangement extends to the liquid based on the strong bonding between the metal and the metalloid in the liquid [35]. The Fe–B complexes are also expected to exist in the amorphous phase. The presence of the Fe_4B phase has not been observed in other studies of crystallization of Fe–B alloys. Its presence may be related to the preparation of the amorphous material in terms of melt temperature or cooling rate, both of which could affect the separation of phases in the liquid as well as in the amorphous phase.

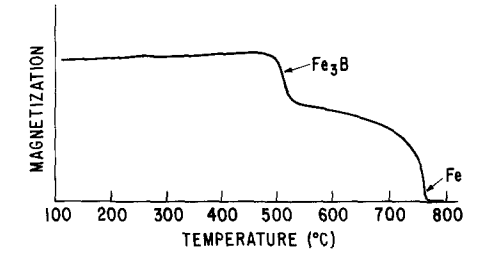

Figure 8 Magnetization of $Fe_{83}B_{17}$ rapidly cooled ribbon during cooling in a field of 51 Oe. Arrows indicate Curie temperatures.

6. Conclusion

Many metastable phases obtained from the amorphous state appear to have compositions and structures which are related to the structures and compositions of the amorphous phase in which they arise. This may occur because it is easier to form a metastable phase than it is to form phases of quite different composition. Thus, in some cases, the amorphous state is shown to be a prerequisite for formation of the metastable phase. In the case of rapid cooling from the melt, the origin of some metastable phases may derive from close packing in the liquid. That is, the chemical short range order in the liquid may survive in the amorphous phase. The metastable Fe_3B phase certainly appears to derive from clusters in the liquid which are present in the amorphous phase in the form of simple unit cells which become the b c tetragonal crystals on annealing. The driving force for clustering in the liquid near the eutectic composition, $Fe_{83}B_{17}$, may be sufficiently great that the Fe_3B phase can exist in crystalline solids cooled at the rate of a few tens or hundred of degrees per minute.

References

1. P. K. SRIVASTAVA, B. C. GIESSEN and N. J. GRANT, *Acta Metall.* **16** (1968) 1199.
2. B. C. GIESSEN, *Adv. X-ray Anal.* **12** (1969) 23.
3. H. JONES, *Rep. Prog. Phys.* **36** (1973) 1425.
4. C. S. CARGILL III, in "Solid State Physics", Vol. 30, edited by F. Seitz, D. Turnball and H. Ehrenreich (Academic Press, New York, 1975) p. 227.
5. D. DUWEZ, *Ann. Rev. Mater. Sci.* 6 (1976) 83.
6. A. K. SINHA, B. C. GIESSEN and D. E. POLK, in "Treatise on Solid State Chemistry", Vol. 3, edited by N. B. Hannay (Plenum, New York, 1976) p. 1.

7. D. E. POLK and B. C. GIESSEN, in "Metallic Glasses" (American Society for Metals, New York 1978).
8. E. M. BREINAN, B. H. KEAR and C. M. BANAS, *Phys. Today* **29** (1976) 11.
9. H. DEWAARD and L. C. FELDMAN, in "Applications of Ion Beams to Metals", edited by S. T. Picraux, E. P. EerNisse and F. L. Vook (Plenum, New York, 1974) p. 317.
10. J. M. POATE, *J. Vac. Sci. Technol.* **15** (1978) 1636.
11. S. MADER, A. S. NOWICK and H. WIDMER, *Acta Metall.* **15** (1967) 203.
12. W. A. GRANT, *J. Vac. Sci. Technol.* **15** (1978) 1644.
13. G. MARCHAL, PH. MANGIN and CHR. JANOT, *Phil. Mag.* **42B** (1980) 81.
14. B. X. LIU and M. -A. NICOLET, *Thin Solid Films* **10** (1983) 201.
15. B. Y. TSAUR, J. W. MAYER and K. N. TU, *J. Appl. Phys.* **51** (1980) 5326.
16. B. Y. TSAUR, J. W. MAYER, M. -A. NICOLET and K. N. TU, "Ion Implantation Metallurgy", edited by C. M. Preece and J. K. Hirvonen (Met. Soc. AIME, Warrendale, Pennsylvania, 1980) p. 142.
17. L. M. HOWE and M. H. RAINVILLE, *J. Nucl. Mater* **68** (1977) 215.
18. W. G. JOHNSTON, A. MOGRO-CAMPERO, J. L. WALTER and H. BAKHRU, *Mater. Sci. Eng.* **55** (1982) 121.
19. R. M. WAGHORN, V. G. RIVLIN and G. I. WILLIAMS, *J. Phys. Metal Phys.* **6** (1976) 147.
20. P. RAMACHANDRARO and T. R. ANATHARAMAN, *Trans. Ind. Inst. Metals.* **23** (1970) 58.
21. T. MASUMOTO and R. MADDIN, *Acta Metall.* **19** (1971) 725.
22. M. TENHOVER, B. M. CLEMENS and P. DUWEZ, *J. Phys. Metal Phys.* **12** (1982) L167.
23. S. ALEXANDER and J. MCTAGUE, *Phys. Rev. Lett.* **41**(1978) 702.
24. J. L. WALTER, *J. Non-Cryst. Solids* **44** (1981) 195.
25. M. HANSEN, "Constitution of Binary Alloys" (McGraw-Hill, New York, 1958) p. 692.
26. J. L. WALTER and S. F. BARTRAM, "Rapidly Quenched Metals III", Vol. 1 (The Metals Society, London, 1978) p. 307.
27. J. L. WALTER, S. F. BARTRAM and R. R. RUSSELL, *Met. Trans.* **9A** (1978) 803.
28. T. HAMADA and F. E. FUJITA, *Jpn. J. Appl. Phys.* **21** (1982) 981.
29. J. L. WALTER, S. F. BARTRAM and I. MELLA, *Mater. Sci. Eng.* **36** (1978) 193.
30. A. E. BERKOWITZ and J. L. WALTER, *ibid.* **55** (1982) 275.
31. J. L. WALTER, A. E. BERKOWITZ and E. F. KOCH, *ibid.* **60** (1983) 31.
32. A. E. BERKOWITZ, J. L. WALTER and K. F. WALL, *Phys. Rev. Lett.* **46** (1981) 1484.
33. S. AUR, T. EGAMI, A. E. BERKOWITZ and J. L. WALTER, *Phys. Rev.* **26B** (1982) 6355.
34. P. DUHAJ and F. HANIC, *Phys. Status Solidi* **76** (a) (1983) 467.
35. H. S. CHEN, *Mater. Sci. Eng.* **23** (1976) 151.

Received 2 July
and accepted 10 July 1984